IEEE Photonics Journal
An IEEE Photonics Society Publication

Open Access

Simultaneous Radio-Frequency and Baseband Signal Transmission Over a Multimode Fiber

Volume 11, Number 6, December 2019

Tatsuya Ohtsuki
Takamitsu Aiba
Motoharu Matsuura, ***Senior Member, IEEE***

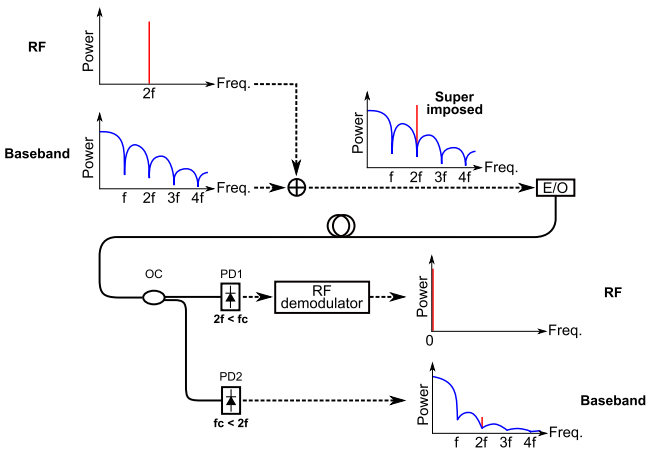

DOI: 10.1109/JPHOT.2019.2957066

Simultaneous Radio-Frequency and Baseband Signal Transmission Over a Multimode Fiber

Tatsuya Ohtsuki,[1] Takamitsu Aiba,[2] and Motoharu Matsuura,[1] *Senior Member, IEEE*

[1]Graduate School of Informatics and Engineering, University of Electro-Communications, Tokyo 182-8585, Japan
[2]Yazaki Corporation, Kanagawa 239-0847, Japan

DOI:10.1109/JPHOT.2019.2957066

Manuscript received October 11, 2019; revised November 19, 2019; accepted November 26, 2019. Date of publication December 2, 2019; date of current version December 17, 2019. Corresponding author: Motoharu Matsuura (e-mail: m.matsuura@uec.ac.jp).

Abstract: We present a simultaneous radio-frequency (RF) and high-speed baseband signal transmission using an electrically superimposed method over a graded-index silica multimode fiber (GI-MMF). To show the feasibility of the method, we experimentally demonstrate simultaneous transmission of electrically superimposed 28-GHz RF and 28-Gbit/s 4-level pulse amplitude modulation (PAM-4) baseband signals at a wavelength of 850 nm over a 50-m GI-MMF. Moreover, to evaluate the scalability of the method, we demonstrate simultaneous transmission of dual-channel, electrically superimposed 28-GHz RF and 14-Gbit/s non-return-to-zero on-off keying baseband signals at 850 nm and electrically superimposed 14-GHz RF and 14-Gbit/s PAM-4 baseband signals at 1550 nm over the 50-m GI-MMF. These results show that the presented method is useful for effectively utilizing the transmission band of transmitters and existing short-reach transmission systems.

Index Terms: Radio-over-fiber (RoF), 4-level pulse amplitude modulation (PAM-4), mobile communications, electrically superimposed transmission, in-home networks, multi-mode fibers (MMFs).

1. Introduction

Recently, internet traffic generated by wireless devices has been increasing rapidly. According to the Cisco Visual Networking Index Forecast, the data traffic of mobile and wireless local area networks will comprise more than half of the global IP traffic in 2021 [1]. As the main part of the data traffic is generated by smartphones and tablets, they must be connected to outdoor as well as indoor locations such as in-home networks. To provide a broader frequency band, super-high frequency (3 to 30 GHz) bands will be used for the next fifth generation (5G) mobile network. In addition, the accelerating demand for broadband wired service using high-speed baseband signals such as on-off-keying (OOK) and 4-level pulse amplitude modulation (PAM-4) signals, makes them indispensable for future wired in-home networks. Hence, simultaneous wired and wireless transmission using a simpler and more cost-effective solution will be a key technology to provide wired and wireless multi-services in such networks.

Radio-over-fiber (RoF) is a promising approach to deliver higher radio-frequency (RF) signals and high-speed baseband signals over optical fibers. In particular, the use of graded-index silica multimode fibers (GI-MMFs) provides a cost-effective solution [2]–[4]. In addition, simultaneous

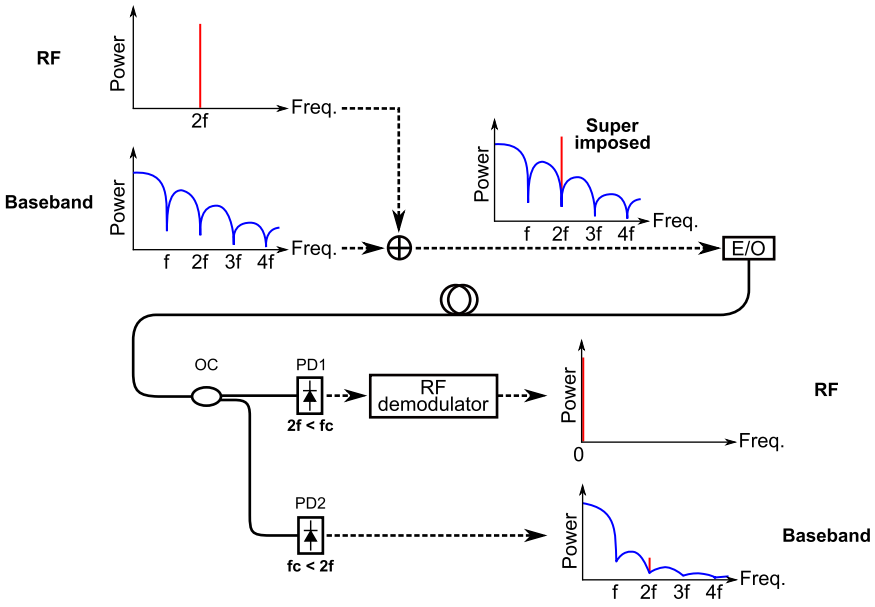

Fig. 1. Operation principle of simultaneous transmission of electrically superimposed RF and baseband signals over an optical fiber. E/O: Electrical-to-optical conversion, OC: Optical coupler, PD: Photo-diode.

RF and baseband signal transmission systems have attracted much attention [5]–[11], because it provides wired and wireless multi-services using a single transmitter and optical fiber. In the electrically superimposed methods [5]–[10], it is important to mitigate crosstalk between RF and baseband signals in the electrical domain, because the bandwidth of baseband signals, such as OOK and PAM-4 signals, is much broader than those of RF signals. Thus, the bit-rate of baseband signals has to be much lower than the carrier frequency of RF signals. In Refs. [8] and [9], to effectively superimpose electrical RF and baseband signals, a specific coding and complicated baseband structure were used. As a result, the additional encoder and decoder were needed, and the available electrical bandwidth generated by the specific coding for inserting RF signals was strictly limited. Although optically superimposed methods using a single transmitter and optical fiber also have been reported [11], [12], complicated transmitters and receivers, including multiple-arms Mach-Zehnder modulators and narrow-band filters are needed.

In this work, we demonstrate simultaneous transmission of a RF signal and a baseband signal using a single transmitter and optical fiber. To effectively superimpose these signals, the carrier frequency of the RF signal is simply located at a broadband spectrum dip of the baseband signal. First, to show the feasibility of the method, we demonstrate simultaneous transmission of electrically superimposed 28-GHz RF and 28-Gbit/s PAM-4 baseband signals at 850 nm over a conventional 50-m GI-MMF. After that, to evaluate the scalability of the method, we also demonstrate simultaneous transmission of dual-channel, electrically superimposed 28/14-GHz RF signals at 850 nm and 14-Gbit/s OOK/PAM-4 baseband signals at 1550 nm over the 50-m GI-MMF.

2. Operation Principle

The operation principle of the simultaneous transmission of electrically superimposed RF and baseband signals over an optical fiber is shown in Fig. 1. An electrical RF signal has narrow bandwidth, while an electrical baseband signal has much broader bandwidth. Thus, when these signals are electrically superimposed in electrical domain, a baseband signal must have a much lower repetition frequency (bit-rate) than the carrier frequency of an RF signal in order to avoid significant crosstalk between the RF and baseband signals [5]–[7], [9]. On the other hand, the

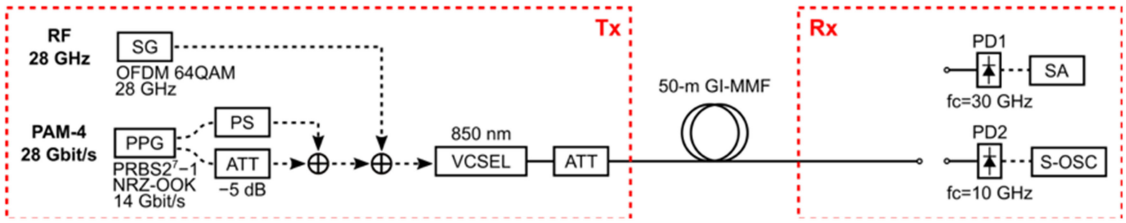

Fig. 2. Experimental setup for multiband transmission of electrically superimposed RF and baseband signals. SG: Signal generator, PPG: Pulse pattern generator, PS: Phase shifter, ATT: Attenuator, VCSEL: Vertical cavity surface emitting laser, GI-MMF: Graded-index silica multimode fiber, SA: Signal analyzer, S-OSC: Sampling oscilloscope.

electrical spectrum of baseband signals has a periodical dip, which is determined by the repetition frequency *f*. In addition, the spectrum has lower power components at higher frequency side, which is easy to insert an RF signal in one of the dips of the spectrum. In our presented method, by fitting the carrier frequency *2f* of an RF signal with the second low frequency spectrum dip of a baseband signal, it is possible to use effectively the signal bandwidth in electrical domain. After converting the superimposed RF and baseband signals into the optical signal and transmitting into an optical fiber, the transmitted signal is converted into the electrical signals by using two photo-diodes (PDs) with each different cut-off frequency *f*c. PD1 has a higher cut-off frequency than the carrier frequency of the RF signal, while PD2 has a lower cut-off frequency than the carrier frequency of the RF signal. In PD1, the RF and baseband signals are detected without the significant bandwidth limitation. After that, in an RF demodulator with direction conversion scheme, the detected RF signal is down-converted after through a band pass filter, and the frequency of the RF signal falls close to a direct current (DC) component with a low pass filter. Then, the frequency components lower than the RF signal disappear, while the frequency components higher than the RF signal are removed in the direct conversion. Thus, the spectrum component of the RF signal is effectively extracted even if there is residual spectrum component of the baseband signal. Conversely, in PD2, only the baseband signal component is detected by the bandwidth limitation, which is determined by the cut-off frequency of PD2. In this way, the electrically superimposed RF and baseband signals are simultaneously transmitted into an optical fiber, and divided by two PDs with each different cut-off frequency without any additional RF components such as electrical lowpass filers.

3. Transmission of Electrically Superimposed 28-GHz RF and 28-Gbit/s PAM-4 Baseband Signals

3.1 Experimental Setup

Fig. 2 shows the experimental setup for multiband transmission of electrically superimposed RF and baseband signals. In the transmitter, a 28-Gbit/s PAM-4 electrical baseband signal was generated using a pulse pattern generator (PPG) with a pseudorandom bit sequence (PRBS) of 2^7–1, while a 28-GHz RF signal based on pre-5G modulation standard: orthogonal frequency division multiplexing (OFDM), 64-quadrature amplitude modulation (64-QAM) format with a signal bandwidth of 90 MHz, and modulation and coding scheme 11 (MCS11) was generated using a signal generator (SG). The number and spacing of the OFDM subcarrier were 1201 and 75 kHz, respectively. These signals were combined by commercially available electrical combiners (Keysight Technologies, Inc., 87302C) and injected into a commercially available vertical cavity surface emitting laser (VCSEL) with a cut-off frequency of 18-GHz. The output wavelength of the VCSEL was 850 nm. The insertion loss of the combiner at a frequency of 28 GHz was approximately 7 dB. The optical data signal directly modulated by the VCSEL was transmitted into a 50-m conventional GI-MMF (OM2) with a core diameter of 50 μm. The link length was limited to 50 m due to the transmission bandwidth of the GI-MMF. The relative frequency response to the

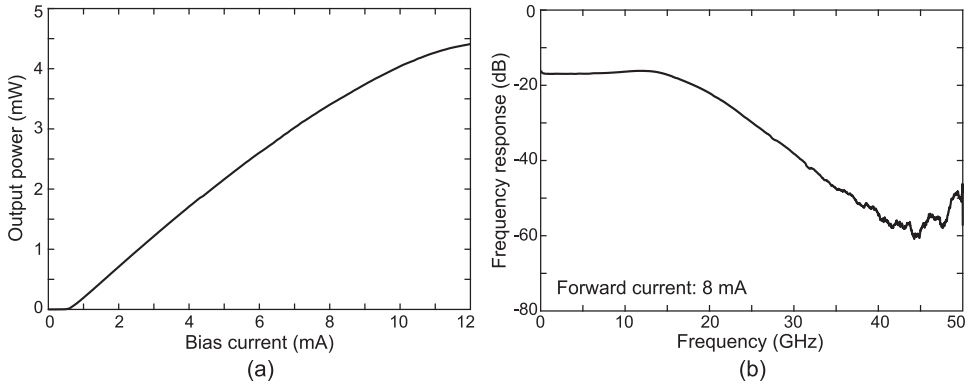

Fig. 3. (a) I-L characteristics and (b) frequency response of VCSEL at forward current of 8 mA.

back-to-back of the 50-m GI-MMF at a frequency of 28 GHz was approximately 1.9 dB lower than that of the back-to-back. The signal power injected into photodiodes (PDs) was fixed at +2.7 dBm by adjusting the attenuation of an optical attenuator (ATT) at the input of the 50-m GI-MMF. The transmitted signal was detected by one of the two PDs (PD1 and PD2). With a cut-off frequency of 30 GHz, which was higher than the carrier frequency of the RF signal, PD1 was used for evaluating the transmission performance of the electrically superimposed 28-GHz RF signal by using a signal analyzer (SA) in terms of the error-vector magnitude (EVM). With a cut-off frequency of 10 GHz, which was much lower than the carrier frequency of the RF signal, PD2 was used for evaluating the transmitted signal quality of the 28-Gbit/s PAM-4 signal by using a sampling oscilloscope (S-OSC) in terms of the eye-pattern. As mentioned in the previous Section, the difference in the cut-off frequency of the PDs is sufficient to separate the RF and baseband signals without using electrical lowpass filters at the outputs of the PDs.

3.2 Experimental Results

Fig. 3(a) shows the I-L (Injection-current Laser-output) characteristics of the VCSEL we used. The I-L curve had high linearity in the range between 2 mA and 11 mA, and was suitable for analog modulation such as RF signals and PAM-4 signals. The forward current was set to 8 mA in the following experiment. The frequency response of the VCSEL at a forward current of 8 mA is shown in Fig. 3(b). Although the frequency of 28 GHz had large degradation due to the frequency response, it was possible to transmit the 28-GHz RF signal with the 28-Gbit/s PAM-4 signal over the 50-m GI-MMF.

Fig. 4 shows the electrically superimposed spectrum of the 28-GHz RF and 28-Gbit/s PAM-4 baseband signals before injecting into the 850 nm VCSEL and after electrical-to-optical (E/O) conversion by the VCSEL and optical-to-electrical (O/E) conversion by the PD1 without the 50-m GI-MMF transmission, based on the setup as shown in Fig. 2. In this measurement, the transmitter was directly connected to PD1 without inserting the 50-m GI-MMF. In Fig. 4(a), the 28-GHz RF signal with a bandwidth of 90 MHz was inserted at the second spectrum dip of the 28-Gbit/s PAM-4 signal to mitigate the crosstalk between the RF and baseband signals. After E/O and O/E conversions, there were two significant changes. One change was that a large spectrum component was appeared at around the first spectrum dip (14 GHz) of the 28-Gbit/s PAM-4 signal, as shown in the arrow of Fig. 4(b). The spectrum dip at 14 GHz was mainly induced during the E/O conversion process owing to the nonlinearity of I-L characteristics of the VCSEL. The other change was that the spectrum component was drastically decreased at the higher frequency range. This was caused by the bandwidth limitation of the VCSEL, with a cut-off frequency of 18-GHz. As shown in Fig. 4(b), the bandwidth limitation was sufficient to reduce the spectrum component of

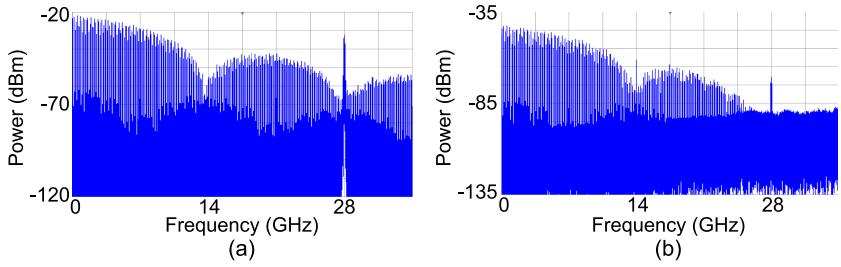

Fig. 4. Electrically superimposed spectrum of 28-GHz RF and 28-Gbit/s PAM-4 baseband signals (a) before injecting into 850 nm VCSEL and (b) after E/O and O/E conversions without 50-m GI-MMF transmission.

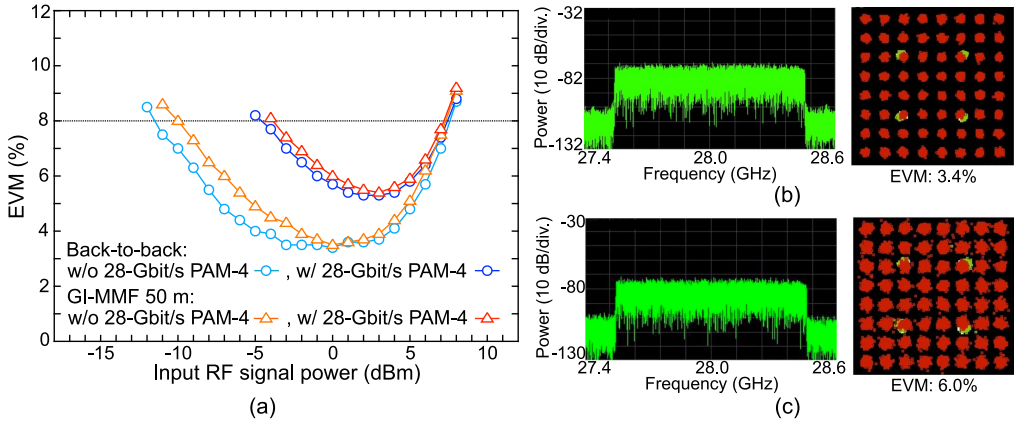

Fig. 5. (a) EVM characteristics of back-to-back and transmitted 28-GHz RF signals over 50-m GI-MMF while varying input RF signal power to the VCSEL. (b) Electrical signal spectrum and constellation of back-to-back signal without 28-Gbit/s PAM-4 signal when input RF signal power was 0 dBm. (c) Electrical signal spectrum and constellation of transmitted signal over 50-m GI-MMF with 28-Gbit/s PAM-4 signal when input RF signal power was +3 dBm.

the 28-Gbit/s PAM-4 signal at the higher frequency range. As a result, the 28-GHz RF signal, not including the large spectrum component of the 28-Gbit/s PAM-4 signal could be detected by PD1. In other words, the spectrum component of the RF signal could be effectively extracted even if there were residual spectrum components of the baseband signal.

Fig. 5(a) shows the EVM characteristics of the back-to-back and transmitted 28-GHz RF signals over the 50-m GI-MMF, while varying the input RF signal power to the VCSEL. The dashed line shows the EVM value of 8%. For 64-QAM signals, the EVM value needs to be less than 8% [13]. Here, the peak-to-peak voltage of the PPG output was set to 800 mVpp. In both cases, it could be observed that the signal quality of the RF signal was degraded by superimposing the 28-Gbit/s PAM-4 baseband signal. The electrical power penalties between with and without the baseband signal of the back-to-back and transmitted signals at the EVM of 8% (dotted line) were approximately 7.0 dB and 6.0 dB, respectively. The dynamic ranges of the back-to-back and transmitted signals with the 28-Gbit/s PAM-4 baseband signals at the EVM of 8% were 12.0 dB and 11.0 dB, respectively. Figs. 5(b) and (c) show the electrical signal spectra and the constellations of the back-to-back signal without the 28-Gbit/s PAM-4 signal and the transmitted signal over the 50-m GI-MMF with the 28-Gbit/s PAM-4 signal. These signals had high signal-to-noise ratios (SNRs) and good signal constellation diagrams. In this scheme, the RoF link gain of the 28-GHz RF signal, including the loss of the combiner, was approximately –45 dBm. For example, the SG

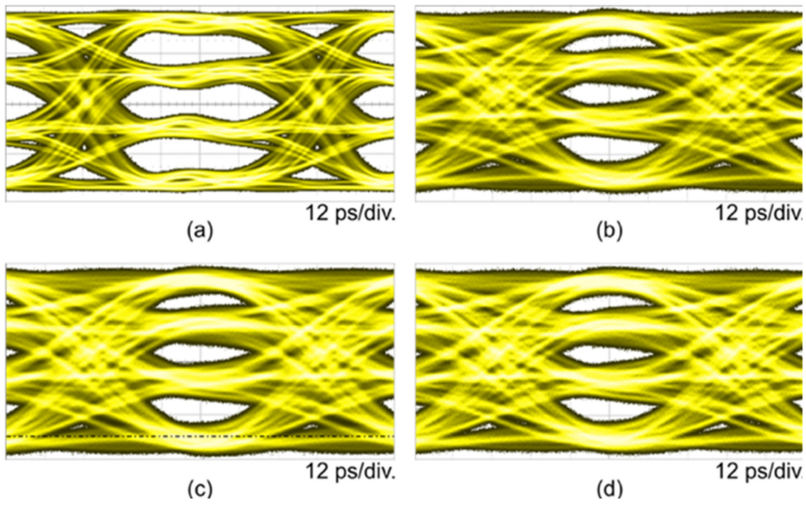

Fig. 6. (a) Eye-pattern of 28-Gbit/s electrical PAM-4 signal w/o RF signal. Eye-patterns of 28-Gbit/s optical PAM-4 back-to-back signal (b) w/o and (c) w/ RF signal and (d) transmitted signal into 50-m GI-MMF w/ RF signal when input RF signal power to the VCSEL was +7.5 dBm.

output power of the 28-GHz RF signal was +3 dBm, the electrical signal power injected into the SA was approximately –42 dBm. The power corresponds to the left most of the EVM characteristics of the transmitted 28-GHz RF signal over the 50-m GI-MMF with the 28-Gbit/s PAM-4 signal, as shown in Fig. 5(a).

To evaluate and compare the transmission performance of the 28-Gbit/s PAM-4 baseband signal, we measured the eye-patterns of the signals when the input RF signal power to the VCSEL was set to +7.5 dBm, as shown in Fig. 6. It was clearly observed that all the eye-patterns had clear eye-openings. These results show that the simultaneous transmission of the electrically superimposed 28-GHz RF signal and 28-Gbit/s PAM-4 signal has good performance over the 50-m GI-MMF.

4. Simultaneous Transmission of Electrically Superimposed 28-GHz RF and 14-Gbit/s OOK Baseband Signals at 850 nm and 14-GHz RF and 14-Gbit/s PAM-4 Signals at 1550 nm

4.1 Experimental Setup

In the previous Section, we showed the single-channel, superimposed method to provide cost-effective, wireless and wired services for an in-home network. On the other hand, in order to provide the services for multiple in-home networks, wavelength-division-multiplexing (WDM) also is among the practical methods used to provide a cost-effective transmission system. Thus, we think that the combination of the electrically superimposed method and WDM transmission is an attractive way. In particular, Coarse WDM transmission systems does not need transmitters with high-precision output wavelength and narrowband filters at receivers, which are sensitive to the temperature change of the devices. Moreover, the wavelength bands of 850 nm and 1550 nm are well-known and commonly used in short- and middle-reach transmission, and it is easy to provide cost-effective components. Therefore, in this Section, to evaluate the scalability of the electrically superimposed method and to increase the transmission capacity over a GI-MMF link, we demonstrated dual-channel transmission of the electrically superimposed RF and baseband signals at 850 nm and 1550 nm. The experimental setup is shown in Fig. 7. In the 850-nm transmitter, a 14-Gbit/s non-return-to-zero OOK electrical baseband signal was generated using a PPG with a PRBS of 2^7–1, while a 28-GHz OFDM, 64-QAM, RF signal with a bandwidth of 90 MHz

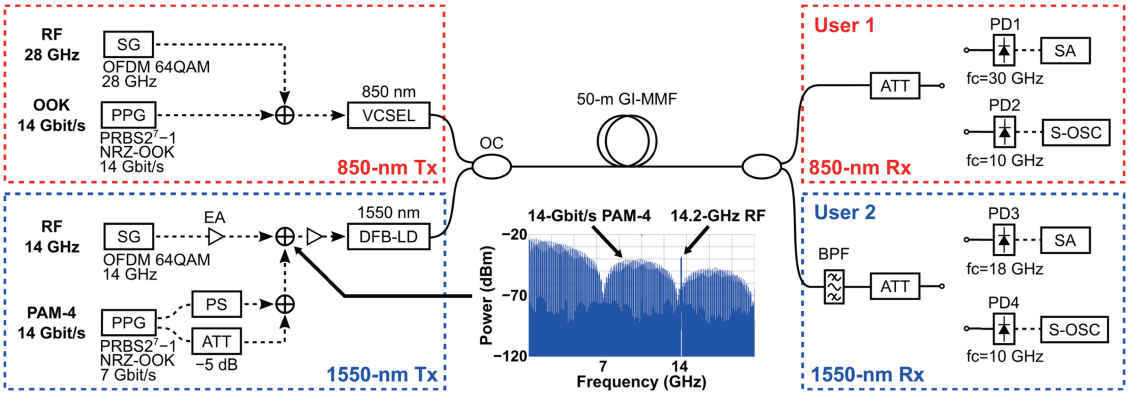

Fig. 7. Experimental setup for multiband transmission of electrically superimposed RF and baseband signals. OC: Optical coupler, EA: Electrical amplifier, DFB-LD: Distributed feedback laser-diode, BPF: Band-pass filter. Inset shows electrical spectrum of electrically-superimposed RF and PAM-4 baseband signals.

was generated using an SG. These signals were combined and injected into the VCSEL we used in the previous experiment. In the 1550-nm transmitter, a 14-GHz RF signal with a bandwidth of 90 MHz and 14-Gbit/s PAM-4 baseband signals were combined and injected into a commercially available distributed-feedback laser-diode (DFB-LD) with a cut-off frequency of 18 GHz. As the DFB-LD required high injection power for the direct modulation, commercially available electrical amplifiers (EAs) whose effective gain is 23 dB in our experiment were used at the output of the SG and the input of the DFB-LD. All the electrical combiners for combining RF and baseband signals were the commercially available combiners (Keysight Technologies, Inc., 87302C), which were same as the previous experiment. In this scheme, the second harmonic component was appeared at the second spectrum dip (14 GHz) of the 14-Gbit/s PAM-4 baseband signal, because the DFB-LD had larger nonlinearity of I-L characteristics than the VCSEL and high cut-off frequency (18 GHz), which was not enough to reduce the spectrum component of the 14-Gbit/s PAM-4 signal at a higher frequency range. Thus, to mitigate the interference between the second harmonic component and the 14-GHz RF signal as weak as possible, the frequency of the 14-GHz RF signal was slightly shifted to 14.2 GHz. After combining the 850-nm and 1550-nm signals using an optical coupler (OC), they were transmitted into the 50-m GI-MMF we used in the previous experiment. The optical powers of the 850-nm and 1550-nm signals injected into the OC were +5.0 dBm and +7.0 dBm, respectively. The transmitted signals were divided using an OC and received at the 850-nm and 1550-nm receivers. In each receiver, an ATT was used to adjust the power injected into the PDs. The received optical power of the 850 nm PDs (PD1 and PD2) and the 1550 nm PDs (PD3 and PD4) were fixed at –1 dBm and –3 dBm, respectively. A bandpass filter (BPF) in the 1550-nm receiver was used to remove the 850-nm signal component, while a BPF in the 850-nm receiver was not used, because the operating wavelength of the PDs was outside the 1550-nm wavelength region. If we can use PDs, which are outside the 850-nm wavelength region, it will be possible to remove the BPF at the input of the 1550-nm receiver. In the 850-nm and 1550-nm receivers, two PDs, each with a different cut-off frequency, were used to extract only one of the electrically superimposed RF and baseband signals. In the 850-nm receiver, the 28-GHz RF and the 14-Gbit/s OOK baseband signals were detected by PD1 with a cut-off frequency of 30 GHz, and the signal quality of the RF signal was measured by a SA in terms of the EVM. Conversely, only the 14-Gbit/s OOK baseband signal was detected by PD2 with a cut-off frequency of 10 GHz, and the eye-pattern of the baseband signal was monitored by an S-OSC. In the 1550-nm receiver, the 14-GHz RF and 14-Gbit/s PAM-4 signals were detected by PD3 with a cut-off frequency of 18 GHz, while only the 14-Gbit/s PAM-4 signal was detected by PD4 with a cut-off frequency of 10 GHz. The actual frequency response of PD2 and PD4 had 30 dB decrease at around 20 GHz, which was useful for

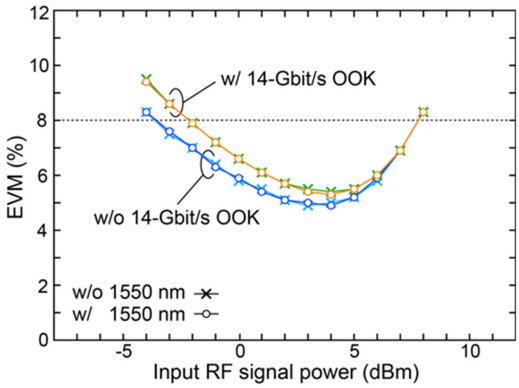

Fig. 8. EVM characteristics of back-to-back 28-GHz RF signals at 850 nm while varying input RF signal power to the VCSEL.

removing the RF signals while passing through the baseband signals after PD2 and PD4 in this experiment. The transmission performance of these signals was measured by a SA and a S-OSC as well as the 850-nm receiver.

4.2 Transmission Performances at 850 nm

To show the feasibility of our proposed method using dual-channel transmission at 850 nm and 1550 nm, we evaluated the transmission performance of the electrically superimposed RF and baseband signals. First, we evaluated the quality of the superimposed signal at 850 nm. Here, the peak-to-peak voltage of the PPG output was set to 300 mVpp. Fig. 8 shows the EVM characteristics of the back-to-back 28-GHz RF signal at 850 nm, while varying the input RF signal power to the VCSEL. It was observed that the electrical power penalties between with and without the multiplexing of the 1550-nm signal of the back-to-back signals at the lower-side input RF signal power at the EVM of 8% were less than 0.1 dB. Conversely, it was observed that the electrical power penalty between with and without the electrically superimposition of the 14-Gbit/s OOK baseband signal was approximately 2.0 dB. Although the degradation was much smaller than the single-channel transmission, as shown in Fig. 5, the lower-side input RF signal powers at the EVM of 8% were drastically increased, because the received optical power of PD1 was decreased for 3.7 dB due to the insertion losses of the OCs, and electrical RF signal power depends on square of received optical power. Thus, the high transmission loss of the GI-MMF link was occurred about 8 dB.

Fig. 9(a) shows the EVM characteristics of the back-to-back and transmitted 28-GHz RF signal over 50-m GI-MMF at 850 nm in the dual-channel transmission at 850 nm and 1550 nm. The dynamic range of the back-to-back signal with and without the 14-Gbit/s OOK baseband signal was 11.5 dB and 10.0 dB, respectively. Conversely, the dynamic range of the transmitted signal with the baseband signal was 9.0 dB. Figs. 9(b) and (c) show the electrical signal spectra and the constellations of the back-to-back signal without the 14-Gbit/s OOK signal and the transmitted signal over the 50-m GI-MMF with the 14-Gbit/s OOK signal. These signals had high SNRs and good signal constellation diagrams.

The eye-patterns of the back-to-back and transmitted 14-Gbit/s OOK baseband signals over 50-m GI-MMF with and without the 28-GHz RF signal at 850 nm are shown in Fig. 10. In these cases, the input RF signal power to the VCSEL was set to $+7.5$ dBm. It could be observed that the signals had clear eye-openings. These results show that the electrically superimposed RF and baseband signals at 850 nm have good transmission performance over the 50-m GI-MMF in the dual-channel transmission at 850 nm and 1550 nm.

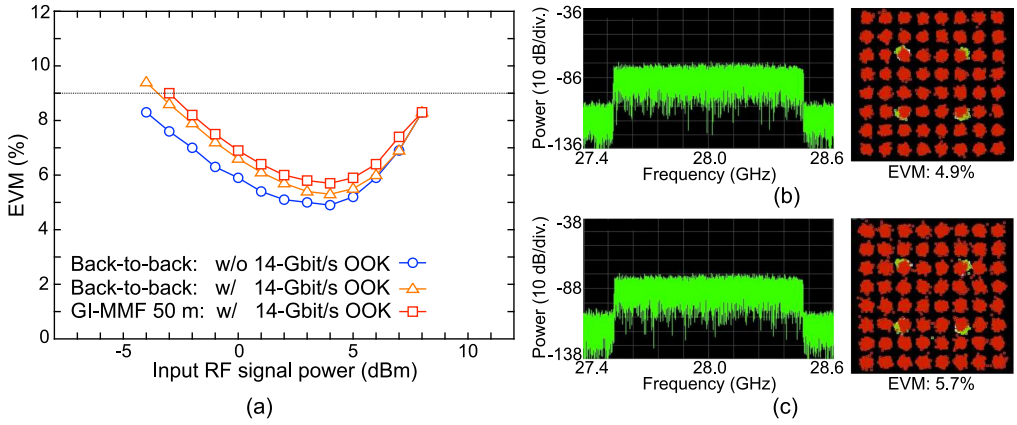

Fig. 9. (a) EVM characteristics of back-to-back and transmitted 28-GHz RF signals over 50-m GI-MMF at 850 nm while varying input RF signal power to the VCSEL. Electrical signal spectra and constellations of (b) back-to-back signal w/o 14-Gbit/s OOK signal and (c) transmitted 28-GHz signal over 50-m GI-MMF w/ 14-Gbit/s OOK signal when input RF signal power was +4 dBm. 4 yellow symbols in each constellation show physical downlink control channel signals to control physical layer.

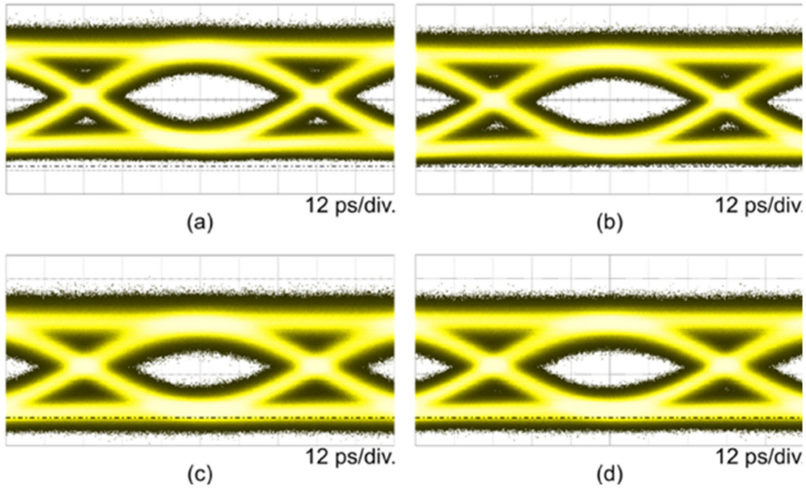

Fig. 10. Eye-patterns of 14-Gbit/s OOK back-to-back signal (a) w/o and (b) w/ RF signal and transmitted signal over 50-m GI-MMF (c) w/o and (d) w/ 28-GHz RF signal when input RF signal power to the VCSEL was 7.5 dBm.

4.3 Transmission Performances at 1550 nm

Fig. 11(a) shows the I-L characteristics of the 1550-nm DFB-LD we used. The I-L curve had high linearity in the range between 10 mA and 140 mA, and was suitable for analog modulation such as RF and PAM-4 signals. The forward current was set to 80 mA in the following experiment. The frequency response of the DFB-LD at a forward current of 80 mA is shown in Fig. 11(b). For the 14-GHz RF and 14-Gbit/s PAM-4 signals, the DFB-LD provides effective modulation performance.

Next, we evaluated the quality of the superimposed RF and baseband signals at 1550 nm. Fig. 12 shows the EVM characteristics of the back-to-back 14-GHz RF signals at 1550 nm, while varying the input RF signal power to the DFB-LD. Because PAM-4 signals have narrower eye intervals compared to OOK signals, the amplitude of PAM-4 signals is significant to provide good transmission performance. Conversely, the amplitude is sensitive not only to the transmission

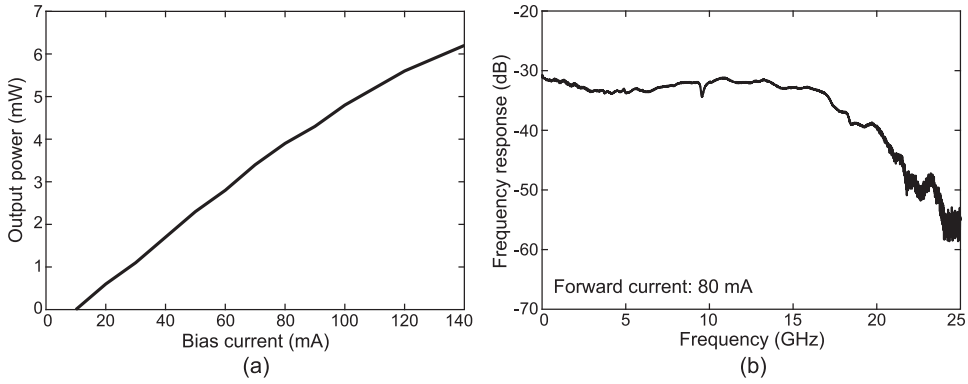

Fig. 11. (a) I-L characteristics and (b) frequency response of DFB-LD at forward current of 80 mA.

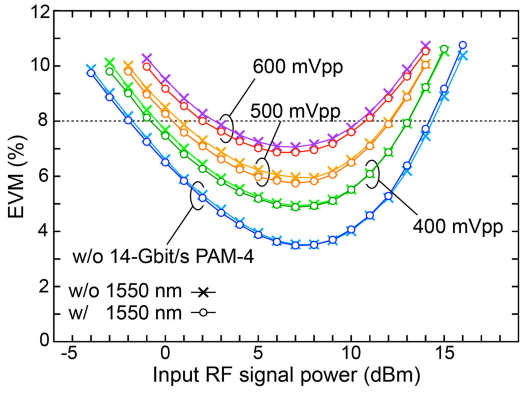

Fig. 12. EVM characteristics of back-to-back 14-GHz RF signals at 1550 nm while varying input RF signal power to the DFB-LD.

performance, but also to the signal quality of the superimposed RF signal. Thus, in this experiment, we investigated the performance related to the amplitude of the 14-Gbit/s PAM-4 signal. In the 1550-nm transmission, it was observed that the quality of the 14-GHz RF signal was minimally degraded by multiplexing of the 850-nm signal. Although the dynamic range of the 14-GHz RF signal was decreased as the amplitude of the 14-Gbit/s OOK baseband signal was increased, more than a 10-dB dynamic range at the EVM of 8% could be obtained at the peak-to-peak voltage of 500 mVpp. Thus, the peak-to-peak voltage was set to 500 mVpp in the following experiment. In addition, it is clarified that the RoF link gain of the 14-GHz RF signal was approximately –55 dBm at without OOK baseband signal condition in this scheme.

Fig. 13(a) shows the EVM characteristics of the back-to-back and transmitted 14-GHz RF signals over 50-m GI-MMF at 1550 nm in the dual-channel transmission at 850 nm and 1550 nm. The dynamic ranges of the back-to-back RF signal with and without the 14-Gbit/s PAM-4 baseband signal and the transmitted RF signal with the baseband signal were 16.0 dB, 11.5 dB, and 7.5 dB, respectively. Compared to the EVM characteristics in the 850-nm transmission, the quality of the RF signals was significantly degraded by superimposing the baseband signals, because the amplitude of the 14-Gbit/s PAM-4 baseband signal was larger than that of the 14-Gbit/s OOK baseband signal at 850 nm. In addition, unlike the 850-nm transmission, the EVM curves did not converge at the larger output signal power side. We suppose that this was caused by the input/output linearity generated by the combination of the cascaded EAs and the DFB-LD, which was different from that of the VCSEL we used. Figs. 13(b) and (c) show the electrical signal spectra and the constellations

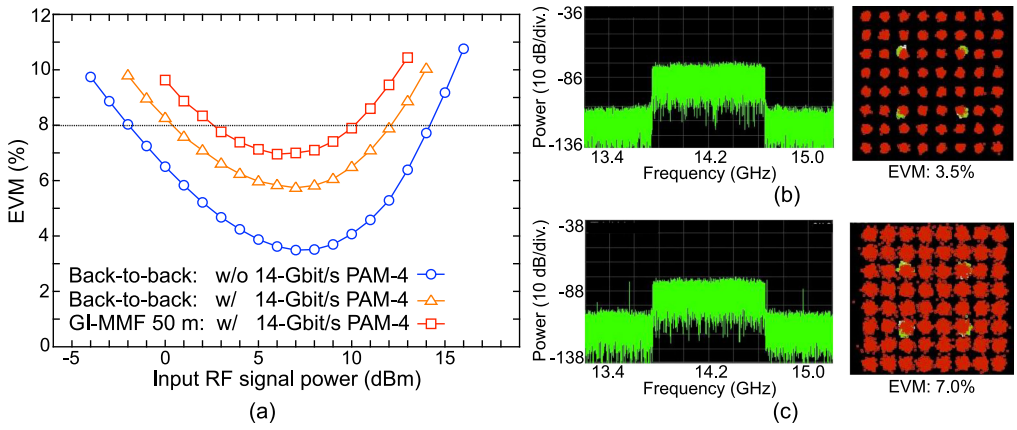

Fig. 13. EVM characteristics of back-to-back and transmitted 14-GHz RF signals over 50-m GI-MMF at 1550 nm while varying input RF signal power to the DFB-LD. Electrical signal spectra and constellations of (b) back-to-back signal w/o 14-Gbit/s PAM-4 signal and (c) transmitted 14-GHz RF signal over 50-m GI-MMF w/ 14-Gbit/s PAM-4 signal when input RF signal power was +7 dBm.

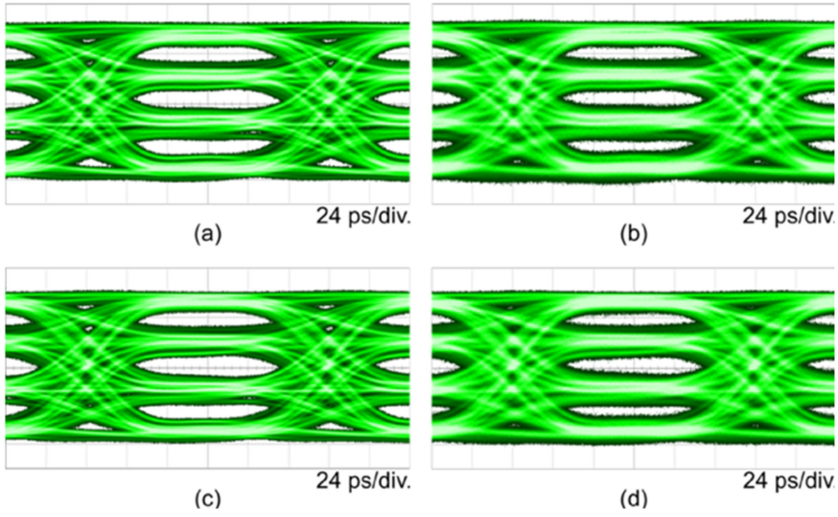

Fig. 14. Eye-patterns of back-to-back 14-Gbit/s PAM-4 signal (a) w/o and (b) w/ 14-GHz RF signal and transmitted 14-Gbit/s PAM-4 signal over 50-m GI-MMF (c) w/o and (d) w/ 14-GHz RF signal when input RF signal power to the DFB-LD was +2 dBm.

of the back-to-back RF signal without the 14-Gbit/s PAM-4 signal and the transmitted 14-GHz RF signal over the 50-m GI-MMF with the 14-Gbit/s PAM-4 signal. These signals had high SNRs and good signal constellation diagrams.

Fig. 14 shows the eye-patterns of the back-to-back and transmitted 14-Gbit/s PAM-4 baseband signals over 50-m GI-MMF with and without the 14-GHz RF signal when the input RF signal power to the DFB-LD was set to +2 dBm. The signal qualities of the back-to-back and transmitted baseband signals were slightly degraded by superimposing the 14-GHz RF signal, because the cut-off frequency of PD2 in the 1550-nm receiver was 10 GHz, which was close to the carrier frequency of the RF signal. Thus, if we use a PD with a lower cut-off frequency, the degradation of the 14-Gbit/s PAM-4 baseband signal will be mitigated. After the 50-m GI-MMF transmission, the signal quality of the 14-Gbit/s PAM-4 baseband signal did not change significantly, compared to the back-to-back signal. The obtained results show that the simultaneous RF and baseband signal transmission

using the electrically superimposed method and the dual-channel transmission provides good transmission performance of the multiband RF and baseband signals over short-reach GI-MMFs.

5. Conclusions

We demonstrated simultaneous transmission of electrically superimposed 28-GHz RF and 28-Gbit/s PAM-4 baseband signals at 850 nm over a 50-m GI-MMF. We also demonstrated the dual-channel transmission of electrically superimposed RF and baseband signals at 850 nm and 1550 nm. In both cases, we successfully achieved good transmission performance and showed that combining of the electrically superimposed method and coarse WDM transmission is an effective and practical means to transmit RF signals and greater than 10-Gbit/s baseband signals over GI-MMFs. The results indicate that the system is useful for future in-home networks.

References

[1] Cisco Inc., "The Zettabyte Era: Trends and analysis," Cisco, San Jose, CA, USA, Tech. Rep. C11-739110-00, 2017.
[2] M. Y. W. Chia, B. Luo, M. L. Yee, and E. J. Z. Hao, "Radio over multimode fibre transmission for wireless LAN using VCSELs," *Electron. Lett.*, vol. 39, pp. 1143–1144, 2003.
[3] A. M. J. Koonen and M. G. Larrode, "Radio-over-MMF techniques—Part II: Microwave to millimeter-wave systems," *J. Lightw. Technol.*, vol. 26, no. 15, pp. 2396–2408, Aug. 2008.
[4] P. Hartmann, X. Qian, A. Wonfor, R. V. Penty, and I. H. White, "1-20 GHz directly modulated radio over MMF link," in *Proc. Int. Top. Meeting Microw. Photon.*, 2005, pp. 95–98.
[5] K. Ikeda, T. Kuri, and K. Kitayama, "Simultaneous three-band modulation and fiber-optic transmission of 2.5-Gb/s baseband, microwave-, and 60-GHz-band signals on a single wavelength," *J. Lightw. Technol.*, vol. 21, no. 12, pp. 3194–3202, Dec. 2003.
[6] C. K. Sim, M. L. Yee, B. Luo, L. C. Ong, and M. Y. W. Chia, "Performance evaluation for wireless LAN, Ethernet and UWB coexistence on hybrid radio-over-fiber picocells," in *Proc. Opt. Fiber Commun. Conf.*, 2005, Paper JWA60.
[7] D. Visani *et al.*, "Wired and wireless multiservice transmission over 1 mm-core GI-POF for in-home networks," *Electron. Lett.*, vol. 47, pp. 203–205, 2011.
[8] C. Chen, M. J. Crisp, R. V. Penty, and I. H. White, "Transmission of simultaneous 10 Gb/s Ethernet and radio-over-fibre transmission using in-band coding," in *Proc. Opt. Fiber Commun. Conf.*, 2013, Paper OM3D.1.
[9] C. Browning *et al.*, "5G wireless and wired convergence in a passive optical network using UF-OFDM and GFDM," in *Proc. IEEE Int. Conf. Commun. Workshops*, 2017, pp. 386–392.
[10] F. Forni, Y. Shi, N. C. Tran, H. P. A. van den Boom, E. Tangdiongga, and A. M. J. Koonen, "Multiformat wired and wireless signals over large-core plastic fibers for in-home network," *J. Lightw. Technol.*, vol. 36, no. 16, pp. 3444–3452, Aug. 2018.
[11] C. T. Lin *et al.*, "Hybrid optical access network integrating fiber-to-the-home and radio-over-fiber systems," *Photon. Technol. Lett.*, vol. 19, pp. 610–612, 2007.
[12] Z. Jia, J. Yu, A. Chowdhury, G. Ellinas, and G.-K. Chung, "Simultaneous generation of independent wired and wireless services using a single modulator in millimeter-wave-band radio-over-fiber systems," *Photon. Technol. Lett.*, vol. 19, pp. 1691–1693, 2007.
[13] 3GPP, "Base Station (BS) radio transmission and reception," Technical Specification Group Radio Access Network, Sophia Antipolis, France, Release 11.2; 3GPP TS 36.104 V11.2, 2012.